

# Classical JAK2V617F+ Myeloproliferative Neoplasms emergence and development based on real life incidence and mathematical modeling

Ana Fernández Baranda<sup>1</sup>, Vincent Bansaye<sup>1</sup>, Evelyne Lauret<sup>2</sup>, Morgane Mounier<sup>3</sup>,  
Valérie Ugo<sup>4</sup>, Sylvie Méléard<sup>\*, 1</sup>, and Stéphane Giraudier<sup>\*, 5</sup>

\* These two authors are co-last authors.

<sup>1</sup>CMAP, Ecole Polytechnique, CNRS, Institut Polytechnique de Paris, Inria, route de Saclay 91128  
Palaiseau, France

<sup>2</sup>Université de Paris, Institut Cochin, INSERM U1016, CNRS UMR8104, F-75014 PARIS, France

<sup>3</sup>Malignant Hemopathies Registry of Cote d'Or, INSERM U1231, CHU Dijon Bourgogne, Dijon, France

<sup>4</sup>Univ Angers, Nantes Université, CHU Angers, INSERM, CNRS, CRCI2NA, F-49000 Angers, France

<sup>5</sup>Université Paris-Cité, Hopital Saint Louis, INSERM U1131, F-75010 Paris, France

**Corresponding author:** Ana Fernández Baranda, ana.fernandez-baranda@polytechnique.edu

**Short title:** Modeling MPN development

**Keywords:** Myeloproliferative Neoplasms, JAK2V617F, EM algorithm

**Fundings:** Funded by the European Union (ERC, SINGER, n°101054787). Views and opinions expressed are however those of the author(s) only and do not necessarily reflect those of the European Union or the European Research Council Executive Agency. Neither the European Union nor the granting authority can be held responsible for them.  
Supported by grants from the INSERM and INCa 2018.

## Abstract

Mathematical modeling allows us to better understand myeloproliferative neoplasms (MPN) emergence and development. We tested different mathematical models on an initial cohort to determine the emergence and evolution times before diagnosis of JAK2V617F classical MPN (Polycythemia Vera (PV) and Essential Thrombocythemia (ET)). We considered the time before diagnosis as the sum of two independent periods: the time (from embryonic development) for the JAK2V617F mutation to occur, not disappear and enter proliferation, and a second time corresponding to the expansion of the clonal population until diagnosis. We demonstrate using progressively complexified models that the rate of active mutation occurrence cannot be constant, but rather increases exponentially with age following the Gompertz model. We found that the first tumorous cell takes an average time of  $63.1 \pm 13$  years to appear and start proliferation. On the other hand, the expansion time is constant: 8.8 years once the mutation has emerged. These results were validated in an external cohort. Using this model, we analyzed JAK2V167F ET versus PV, and obtained that the time of active mutation occurrence for PV takes approximately 1.5 years more than for ET to develop, while the expansion time was similar. In conclusion, our multi-step approach and the ultimate age-dependent model for the emergence and development of MPN demonstrates that the emergence of a JAKV617F mutation should be linked to an aging mechanism, and indicates a 8 – 9 years period of time to develop a full MPN.

# 1 Introduction

Myeloproliferative Neoplasms (MPN) are blood cancers issued from the transformation of hematopoietic stem cell and related to the acquisition of JAK2 signaling deregulation. The most frequent driver mutation in MPN is JAK2V617F, followed by JAK2 exon12, CALR and MPL [1]. MPN are categorized into three main diseases that present the JAK2V617F mutation in the majority of cases: Essential Thrombocythemia (ET), Polycythemia Vera (PV) and Primary Myelofibrosis (PMF) [2]. ET is characterized by an increased platelet number, PV by erythroid compartment enlargement and PMF by bone marrow fibrosis. When the JAK2 mutation is responsible for the pathology development, the mutation is present in one allele for most cells for ET, but often undergoes an homologous recombination of JAK2V617F for PV resulting in the mutation being present in both alleles [3]. In PMF, the JAK2 mutation is often coupled with secondary events such as TET2 mutation or ASXL1 [1]. In order to develop one of these pathologies, two steps are needed: the acquisition of a mutation at stem cell level and the development of the cancerous population. When a diagnosis of MPN just like Polycythemia Vera is performed, the total tumor mass (erythrocytes) represents at least 25% of the erythroid hematopoietic mass [2]. This suggests a total cancer mass of at least 750 grams in the blood and probably the same mass in the bone marrow. Based on the cell mass, we can speculate that a minimum of one million cell divisions are needed to create such a MPN. We also can speculate that the same order or tumor mass is present in all myeloid chronic myeloproliferative malignancies such as ET. Mathematical modelling and statistical analysis through patients data, can help us better understand the dynamics of mutation emergence and expansion, which could yield important information for prevention strategies and early diagnosis.

Two types of data can be found in literature to study the emergence of mutations in HSCs: sequencing data and registries of age of detection. Sequencing data allows to back-track mutations through mathematical models to define the timeline to driver mutation acquisition, (see for example [4], [5], [6]). Detection ages allow to model mutation emergence and expansion as done in [7]. In all of these works around MPN emergence, an assumption of a constant mutation occurrence rate throughout the life of an individual was made. Such an Assumption would imply an exponential distribution for the emergence time (see subsection 3.1). However, the available data (Figure 1) shows a growing number of diagnosed patients for older ages (see also [8] and [9]) whose trend is not consistent with this an exponential. In the present work, we considered registries of age of detection. Once the mutation acquisition time was defined, we studied the time until diagnosis, contrary to [7] were they studied the behaviour of the size of the mutant population.

Using real life registries of MPN and age of pathology detection in patients, we studied the emergence and expansion of MPN for patients presenting the JAK2V617F mutation. Given the reduced number of reported cases for PMF the data does not allow to properly perform statistical analysis. We then centered our study on ET and PV. We defined the time to diagnosis as composed of two elements: the time  $T_1$  of active mutation emergence, namely the time for a first cell harboring the JAK2V617F mutation to emerge and enter the cell cycle, and the time  $T_2$  between emergence and detection, namely the time for cancer population to grow until diagnosis. Then, we presented and tested different models of  $T_1$  and  $T_2$  to better define MPN development. The models studied in this work for the age of detection of MPN can be divided into two categories: ones that consider that the active mutation rate is constant as previously seen in literature, and ones that consider it to be dependent on the age of the individual. The first category of models were analysed under different assumptions and we found that they do not seem to be appropriate to explain significantly (from the statistical point of view) the available data. The second type of models, under the assumption that the active mutation occurrence rate grows with age, suggested a much better fit to the data. Hence, we show that in order to properly explain the two available MPN registries, the active mutation occurrence rate rather than being constant, increases exponentially with age, following a Gompertz distribution, conversely to previous models developed.

## 2 Framework

### 2.1 Incidence and frequencies of MPN according to age

In this study, we used data obtained from the cancer registry of the Côte d’Or in France from 1990 to 2020, which compiles the ages of detection for 264 patients with different types of MPN (Table 1 in Appendix). In this region, life expectancy (and then relative incidence of pathology) can be analyzed. We centered our analysis to patients diagnosed with either PV or TE and presenting the JAK2V617F mutation. The mean detection age in this data set is of 71.9 years with standard deviation of 13.8 years. To further validate the models another set from FIMBANK was used, containing the ages of detection for ET and PV of 1111 individuals as seen in Table 2 in Appendix. In this data set, we have a mean of 64.4 years with a standard deviation of 14.1 years.

The two sets of data used in our analysis were adjusted to take into account the distribution of the population into each age group and consider the proportion of individuals diagnosed within each group. This considers that some individuals could have died before being diagnosed and are thus not present in the data sets. Each frequency was then divided by the probability of survival up to that age group as follows. Let  $T_D$  be the age of death and  $T_M$  the age of detection. Then the frequencies given by the data of the probability of being diagnosed at age  $t$  is given by

$$\mathbb{P}(T_M = t, T_D \geq t).$$

If we suppose independence between the two variables  $T_D$  and  $T_M$ , this is equal to

$$\mathbb{P}(T_M = t)\mathbb{P}(T_D \geq t).$$

Using the death rates for each age group, one can obtain  $\mathbb{P}(T_D \geq t)$  and then calculate

$$\mathbb{P}(T_M = t) = \frac{\mathbb{P}(T_M = t, T_D \geq t)}{\mathbb{P}(T_D \geq t)}.$$

We applied this adjustment based on the French and European survival data by age and sex of 2021 [10]. The resulting corrected data gives us the age distribution of JAK2V617F for patients who have not died of anything else before. This data indicates that the frequencies of JAK2V617F MPN development increases dramatically in older ages as shown in Figure 1. We constructed different models and analyzed their fit with the data.

## 3 Results

### 3.1 Modeling mutation occurrence and mutation expansion: a simple model

In order to perform a diagnosis of PV or ET, the total cancer mass needs to surpass a certain threshold of around  $M = 10^{12}$  cells. We assumed that diagnosis was performed when this size was reached. We consider that the age of detection,  $T_M$ , is the sum of two independent time periods,  $T_1$  and  $T_2$ : the first one being the time from embryonic development for the mutation to occur, not disappear, and enter in proliferation (that we will name “mutation occurrence”) and a second time corresponding to the expansion time, once the first cancer cell begins to proliferate until the time of MPN diagnosis. The times  $T_1$  and  $T_2$  were taken as independent since the time taken for a cell to become proliferative, should not be related to the time for its population to grow to a certain size. In order to consider that the mutation could have appeared at an embryonic level, as suggested in [11],  $T_M$  was considered to start 9 months before the birth of an individual.

To define the first period of time  $T_1$ , we first assumed that the rate of mutation or activation of an existing mutation at stem cell level is constant through the life of the individual and equal to  $\tau$ . Then, the time for a mutation to appear follows an exponential distribution with parameter  $\tau$ . This assumption has been taken in the majority of genetic analysis backtracking reported to date [4], [5], [6]. We considered that each activated mutant cell has a probability  $p$  to proliferate and

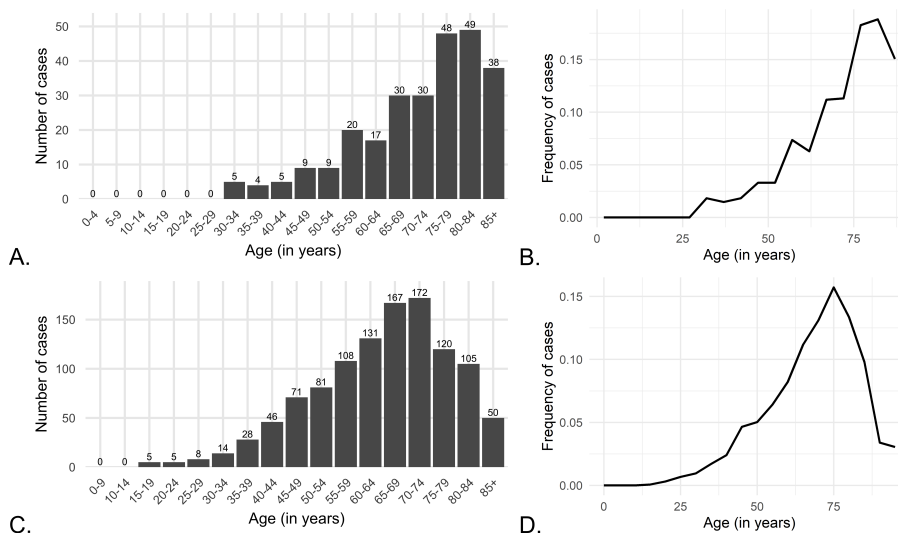


Figure 1: **A**: Incidence by age of JAK2V617F Classical MPN (ET and PV, excluding myelofibrosis) in the Cote d'Or Regional Registry Database. **B**: Incidence by age of JAK2V617F classical MPN (ET and PV, excluding myelofibrosis) in the Cote d'Or Regional Registry Database after adjustment excluding other causes of death before the MPN diagnosis. **C**: Incidence by age of JAK2V617F Classical MPN (ET and PV, excluding myelofibrosis) in the National BCB-FIMBANK Cohort. **D**: Incidence by age of JAK2V617F classical MPN (ET and PV, excluding myelofibrosis) in the National BCB-FIMBANK Cohort after adjustment excluding other causes of death before the MPN diagnosis.

then be detected. The number  $(1 - p)$  corresponds to the frequency of non proliferating mutant cells (just like clonal hematopoiesis does for a long period of time) or of mutant cells whose lineages disappear before reaching detection size of MPN. To find the law of  $T_1$  under these assumptions, let  $L$  be a random variable of law  $Geom(p)$  that corresponds to the number of mutation events before the first active cancer cell appears and let  $X_1, X_2, \dots$  be independent and identically distributed random variables of law  $Exp(\tau)$  that define the time elapsed between two mutation attempts. Then,  $T_1$  will simply be the sum of these times:

$$T_1 = \sum_{i=1}^L X_i.$$

The law of this variable can be found using the generating function

$$\begin{aligned} \mathbb{E} [e^{-\lambda T_1}] &= \mathbb{E} [\mathbb{E} [e^{-\lambda T_1} | L]] = \mathbb{E} \left[ \left( \frac{\tau}{\tau - \lambda} \right)^L \right] \\ &= \sum_{k \leq 1} \left( \frac{\tau}{\tau - \lambda} \right)^k p(1 - p)^{k-1} = \frac{\tau p}{\tau p - \lambda}. \end{aligned}$$

Then,  $T_1$  is an exponential random variable with parameter  $\delta = \tau p$ , and its law is given by

$$f_1(t) = \delta \exp(-\delta t),$$

where  $t \geq 0$  represents the age of an individual.

The time  $T_2$  corresponds to the time taken for a population of cells to reach detection size of  $10^{12}$  cells. Given the high number of divisions needed to reach this size ( $10^6$  divisions), variability in division time is averaged and it makes sense to consider that the expansion time should be similar from one individual to the other. The law of  $T_2$  then needs to be unimodal, centering around a

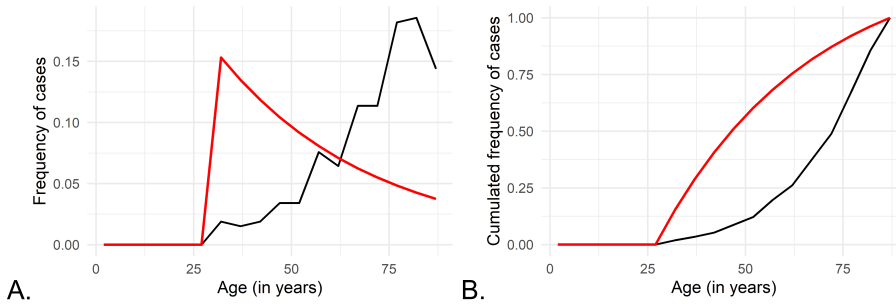


Figure 2: **A**: Frequency of cases for the data (in black) and probability density function of the estimation (in red) for the classical model (1) **B**: Accumulated frequencies of cases for the data (black) and cumulative distribution of the estimation (in red) for the classical model (1)

certain value as for example, a lognormal law. The simplest case is to consider a null variance, where all individuals have the same expansion time, implying that environmental modifications do not have an effect on the growth of the tumor. Following this reasoning, we started by assuming that  $T_2$  was a fixed value  $\alpha$  and later studied the case when  $T_2$  is a lognormal random variable (see Section 3.2).

Then, in our first model the time  $T_M$  for detection age is distributed as a shifted exponential law, that is for  $t \geq \alpha$ ,

$$f_M(t) = \delta \exp(-\delta(t - \alpha)). \quad (1)$$

The shift  $\alpha$  has to be a value between 0 and the minimum age of diagnosis in our cohort. We estimated the parameters  $\delta$  and  $\alpha$  of the model with a least-squared estimation which minimizes the sum of the square difference between the data and our model for each age. Figure 2 illustrates the data of clinical incidence of MPN in real life compared to the estimation, showing a large disparity between the model and the data. The model follows the opposite trend as the data: it gives a strong probability to small ages, while the data is more focused on older ages. It seems that this model is not appropriate given this type of data. To confirm this, we performed a Chi-square goodness-of-fit test to study the hypothesis that the data follow the distribution of our model and found that it was rejected at a 99% significance level with a p-value smaller than  $10^{-17}$ , indicating that a constant occurrence rate together with constant expansion time does not fit with the clinical data.

### 3.2 Relaxed assumptions on mutation emergence or expansion time

In an attempt to properly explain the clinical incidence of MPN in the Côte d'Or cohort, we considered two relaxed models that allow additional types of variability: either individual variability on cancer cell emergence or influence of environment on cancer development.

The first model took into account individual variability allowing the time of mutation occurrence to vary from one patient to another or the mutation to develop at different times from one patient to another (quiescence/cycling). This takes into consideration that the biological hypothesis of stress (or environment) influences cancer cell emergence. This model considered again  $T_2$  as a fixed value  $\alpha$  and  $T_1$  as an exponential random variable, but its rate is different from one patient to another. Then, for  $1 \leq i \leq N$ , where  $N$  is the number of patients, we considered that each age of detection  $Y_i$  is drawn from an exponential distribution with parameter  $\delta_i$ . The  $\delta_i$ 's are considered as an independent sample of a *lognormal*( $m, s^2$ ), which distribution for  $t > 0$  is given by

$$g_\delta(t) = \frac{1}{ts\sqrt{2\pi}} \exp\left(-\frac{(\log(t) - m)^2}{2s^2}\right),$$

where  $t$  represents the age of an individual. This distribution was considered for the  $\delta_i$ 's since it's of positive support and unimodal. As in the previous model, we obtain that the law of  $T_M$

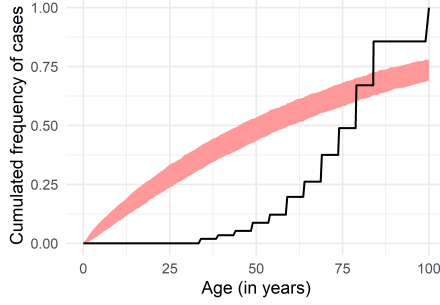


Figure 3: Accumulated frequencies of cases for the data (in black) and 90% confidence interval of the estimation (in red) for the classical model with individual variability (2).

is a shifted exponential distribution (1), but the parameter  $\delta$  is different from one individual to another. Indeed, for individual  $i$ , the distribution of the age of detection  $T_M^i$  is given by

$$f_M^i(t) = \exp(-\delta_i(t - \alpha)). \quad (2)$$

We can then estimate the values of the parameters  $m$ ,  $s$  and  $\alpha$  using the software Monolix [12]. This software is well adapted for this mixed effect modeling as it allows to easily estimate the parameters when considering the survival analysis approach. The estimation is based of the SAEM algorithm and gives robust and global convergence. Figure 3 illustrates the data compared to the approximation. The data presents such a big discrepancy that it is sufficient to reject this model.

A second model considered that external factors may not influence the emergence but rather the expansion time and the time of detection. Then, the mutation occurrence rate of JAK2V617F is fixed and constant while the expansion time of cancer development,  $T_2$  is taken as a random variable. This could be explained by invasion process modifications (ie variation time between two divisions), environment modifications or randomness in the diagnostic process (some patients are diagnosed after vascular events (late detection) when others are diagnosed after a systematic blood cell analysis performed for another pathology (early detection)) or some subjects die (of other unrelated pathologies) before  $T_2$  was finalized. Considering that it has to be similar between individuals,  $T_2$  is taken as a lognormal random variable. The distribution of  $T_2$  is given by

$$f_2(t) = \frac{1}{t\sigma\sqrt{2\pi}} \exp\left(-\frac{(\log(t) - \mu)^2}{2\sigma^2}\right), \quad (3)$$

for  $t > 0$ . Since  $T_1$  and  $T_2$  are considered independent, we then have that the law of the age of detection  $T_M$  has the density for any  $t > 0$

$$\begin{aligned} f_M &= \int_0^t f_1(s)f_2(t-s)ds \\ &= \int_0^t \delta \exp(-\delta s) \frac{1}{(t-s)\sigma\sqrt{2\pi}} \exp\left(-\frac{(\log(t-s) - \mu)^2}{2\sigma^2}\right) ds. \end{aligned} \quad (4)$$

This model combines an exponential random time for mutation occurrence and a lognormal random time for expansion. The parameters  $\delta$ ,  $m$  and  $s$  were estimated through a least-squares estimation. This model was also rejected at 99% confidence level through a Chi-square goodness-of-fit test (Figure 4) with a p-value smaller than  $10^{-17}$ .

The rejection of both of these models imply that even when including individual or environmental variations, models with constant active mutation occurrence  $\delta$  cannot explain the data. Thus, alternative models based on an increasing probability of JAK2V617F cancer cell emergence with age were mandatory.

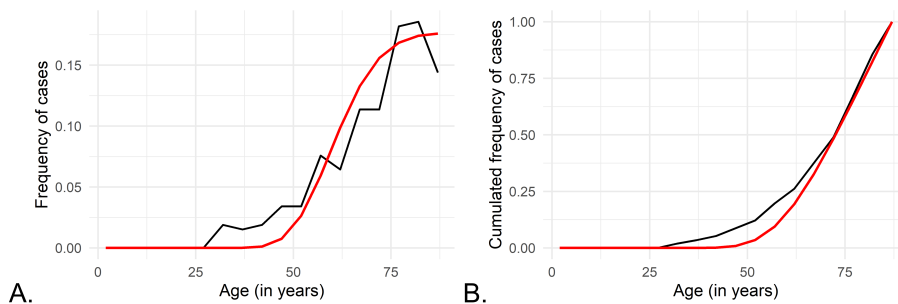


Figure 4: **A**: Frequency of cases for the data (in black) and probability density function of the estimation (in red) for the classical model with lognormal MPN growing time (4). **B**: Accumulated frequencies of cases for the data (in black) and cumulative density of the estimation (in red) for the classical model with lognormal MPN growing time (4).

### 3.3 Age-dependency of JAK2V617F mutation emergence

We consider an active mutation occurrence rate that grows as a person gets older. Biological motivation behind considering an age-dependent mutation occurrence rate can be justified by at least three age-dependent modifications of the environment: i- JAK2V617F mutation appearance (from embryo to adulthood), ii- JAK2V617F activation (ie stem cell quiescence exit) or iii- the success probability of the expansion after activation. Let  $\delta(t)$  be the age-dependent active mutation rate, then the distribution of the emergence time  $T_1$  becomes

$$\hat{f}_1(t) = \delta(t) \exp\left(-\int_0^t \delta(s) ds\right), \quad (5)$$

with  $t$  the age of an individual. We study two classical models used in survival analysis for age-dependent rates: the Gompertz model and the Weibull model (see [12], pages 90-92). For an age  $t$ , the respective functions for the mutation occurrence rate are given by

$$\begin{aligned} \delta_G(t) &= A \exp(kt), & (\text{Gompertz rate}) \\ \delta_W(t) &= \frac{\gamma}{\lambda} \left(\frac{t}{\lambda}\right)^{\gamma-1}, & (\text{Weibull rate}), \end{aligned}$$

where  $A > 0$ ,  $k > 0$ ,  $\gamma > 0$ ,  $\lambda > 0$ . Since the focus is on studying if age dependency on the active mutation rate can explain the data, we consider the broader model with  $T_2$  as a lognormal random variable with density function (3). The addition of variability to the expansion time  $T_2$  should give the same fit or better than a fixed value. We later discuss the case of  $T_2$  constant. Under these assumptions, the law of  $T_M$  is given by

$$\hat{f}_M(t) = \int_0^t \hat{f}_1(s) f_2(t-s) ds,$$

since  $T_1$  and  $T_2$  are independent, with  $\hat{f}_1$  given by (5) and  $f_2$  given by (3) and  $t$  the age of an individual.

For both the Gompertz and Weibull models, we estimated the parameters using the generalized Expectation-Maximization (EM) algorithm (see for example [13]) as presented in [14].

Let us recall the method. Let  $X$  be the vector that corresponds to the observed data of detection ages and has distribution  $f_X(x; \theta)$  for an age  $x$ , where  $\theta$  is the vector of parameters. Consider the missing data  $z$ , corresponding to the values of  $T_2$  with distribution  $f_Z(z; \theta)$ . Then the complete data is  $(x, z)$ , and it is distributed according to  $f_{X,Z}(x, z; \theta)$ . If the complete data was available, the the log-likelihood could be calculated by

$$\log L_{X,Z}(\theta) = \log f_{X,Z}(x, z; \theta).$$

The goal is to find the values of the parameters that maximize this function. This algorithm is iterative and consists of two steps: the E-step and the M-step. Starting from an initial value  $\theta_0$ , then, on iteration  $k + 1$ , the E-step involves computing

$$Q(\theta; \theta_k) = \mathbb{E}_{\theta_k}(\log L_{X,Z}(\theta)|x).$$

Then, on the M-step choose  $\theta_{k+1}$  such that

$$Q(\theta_{k+1}; \theta_k) \geq Q(\theta_k; \theta_k).$$

For the M-step, as suggested in [14], we take  $\theta_{k+1}$  as one Newton-Raphson step from  $\theta_k$  over the function  $Q(\theta_{k+1}; \theta_k)$ , that is

$$\theta_{k+1} = \theta_k + a_k \delta_k,$$

where

$$\delta_k = - \left[ \frac{\partial^2(Q(\theta; \theta_k))}{\partial \theta \partial \theta^T} \right]^{-1} \bigg|_{\theta=\theta_k} \left[ \frac{\partial(Q(\theta; \theta_k))}{\partial \theta} \right] \bigg|_{\theta=\theta_k}$$

and  $0 < a_k \leq 1$ . The choice of  $a_k$  needs to be such that it stays in the parameters space and the likelihood is nondecreasing. To do this, take  $a_k^0 = 1$  and divide by half its value until the parameters satisfy the desired conditions. Then, we apply backtracking line search : while  $Q(\theta_k + a_k \delta_k; \theta_k) > Q(\theta_k; \theta_k) + 10^{-4} a_k \nabla Q(\theta_k; \theta_k)^T \delta_k$ , set  $a_k = 0.8 a_k$ . Then, we take  $a_k$  as the final value of these steps.

Once the parameters estimation was done, we performed a Chi-square goodness-of-fit test to study the hypothesis that the data fits both of the two models. We found that the Weibull model was rejected with a p-value smaller than  $10^{-17}$  and the Gompertz model was not rejected with a power of 0.85, indicating that this model seems to properly explain the data. The Gompertz model has been widely used to model different biological age-dependent rates such as mortality [15] or cancer death rate [16]. In our case, it can be explained as follows: we assume that individuals have an initial mutation occurrence rate  $A$ , and an age-related increase in mutation occurrence represented through a parameter  $k$ . Then, for an age  $t$ , the active mutation occurrence takes the form  $\delta_G(t)$ . Under this hypothesis, the distribution of the time of active mutation emergence  $T_1$  is the following

$$\hat{f}_1(t) = A \exp\left(\frac{A}{k}\right) \exp(kt) \exp\left(-\frac{A}{k} \exp(kt)\right).$$

From (5), we obtain the following distribution for the age of detection  $T_M$

$$\hat{f}_M(t) = \int_0^t A \exp\left(\frac{A}{k}\right) \exp(ks) \exp\left(-\frac{A}{k} \exp(ks)\right) \frac{1}{(t-s)\sigma\sqrt{2\pi}} \exp\left(-\frac{\log(t-s)-\mu}{2\sigma^2}\right) ds, \quad (6)$$

since  $T_1$  and  $T_2$  are assumed to be independent. By applying the EM-algorithm to our data, we obtain the following estimations on the parameters of the model

$$A = 0.000122, \quad k = 0.095814, \quad \nu = 2.083590, \quad \sigma = 0.099585.$$

With these parameters, we obtain that the mean of  $T_2$  is 8.07 years with a standard deviation of 0.81 years.

### 3.4 Age-dependency of JAK2V617F mutation emergence with different models of tumor growth

We obtained in Section 3.3 that the Gompertz model with random expansion time is not rejected. But given the small variance of  $T_2$ , we want to investigate whether a fixed expansion time is sufficient to properly explain the data. When considering  $T_2 = \alpha$ , we obtain the following distribution for the age of detection  $T_M$

$$\hat{f}_M(t) = A \exp\left(\frac{A}{k}\right) \exp(k(t-\alpha)) \exp\left(-\frac{A}{k} \exp(k(t-\alpha))\right). \quad (7)$$

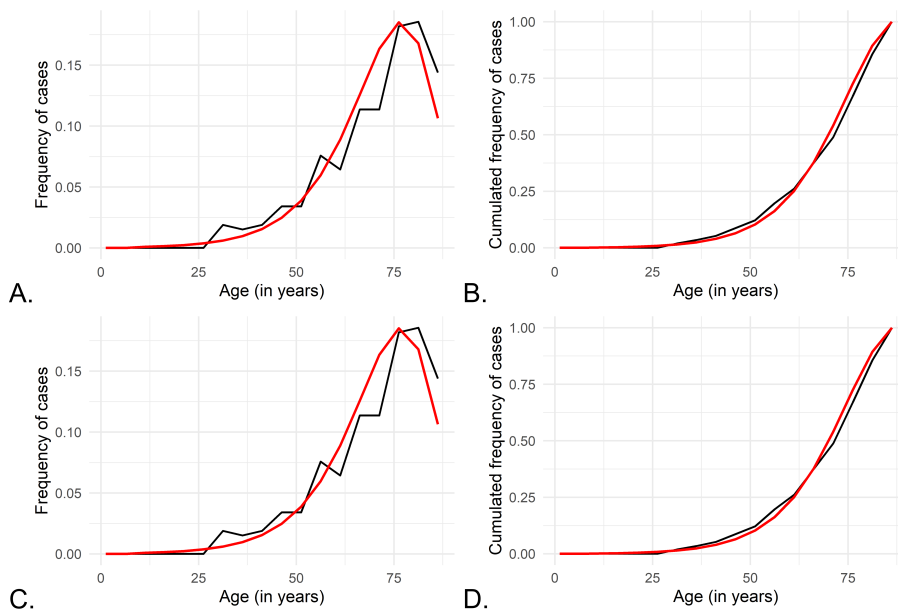


Figure 5: **A**: Frequency of cases for the data (in black) and probability density function of the estimation (in red) for the model with aging (7). **B**: Accumulated frequencies of cases for the data (black) and cumulative distribution of the estimation (in red) for the model with aging (7). **C**: Frequency of cases for the data (in black) and probability density function of the estimation (in red) for the model with aging and lognormal MPN growing time (6) **D**: Accumulated frequencies of cases for the data (black) and cumulative distribution of the estimation (in red) for the model with aging and lognormal MPN growing time (6).

The parameters were estimated using the same EM-algorithm as previously and we obtained the following values

$$A = 0.000124, \quad k = 0.096577, \quad \alpha = 8.76.$$

Using this estimation, a Chi-square goodness-of-fit test resulted in not rejecting this model with a power of 0.952. We refer to Figure 5 for visual comparison between the estimations for fixed  $T_2$  in **A-B** and random  $T_2$  in **C-D**.

Since both models with a Gompertz function for the active mutation occurrence and with a fixed or lognormal expansion time  $T_2$  are not rejected, we use the Bayesian information criterion (BIC) presented in [17] to select the most appropriate model amongst these two to explain the data. This criterion is defined by

$$\text{BIC} = k \log n - 2 \log \mathcal{L},$$

where  $k$  is the number of parameters of the model,  $n$  is the size of the data sample and  $\mathcal{L}$  is the likelihood function. The BIC uses the likelihood function to measure how well a model can explain the data, while also penalizing the number of parameters in the model to avoid overfitting. A lower BIC is preferred. We obtain that the Gompertz model with constant MPN expansion time (7) ( $T_2$  as a fixed value) has a BIC of 2079 and the Gompertz model with lognormal MPN expansion time (6) has one of 2085.3. This indicates that the model with fixed expansion time should be chosen. While incorporating variability on the expansion time  $T_2$  gives a better fit to the data in terms of the likelihood, the gain is small and not compensated by the cost of adding additional parameter to the model. This would imply that, given our data, the Gompertz model with constant MPN expansion time is the most appropriate to explain the data. This suggests that environmental modifications (or other sources of variability) do not have a huge impact on the growth phase of the tumor. Using the estimation of the selected Gompertz model with fixed expansion time, we obtained that the expected occurrence time  $T_1$  is of 63 years with a standard deviation of 13 years

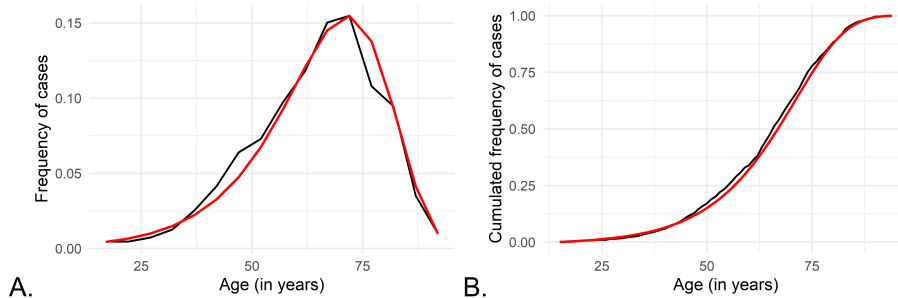


Figure 6: **A:** Incidence by age of JAK2V617F Classical MPN (ET and PV, excluding myelofibrosis) in the National BCB-FIMBANK Cohort. **B:** Incidence by age of JAK2V617F classical MPN (ET and PV, excluding myelofibrosis) in the National BCB-FIMBANK Cohort after adjustment excluding other causes of death before the MPN diagnosis.

and the pathology development when the first JAK2V617F stem cell is present, fixed and ready to proliferate is 8.8 years ( $T_2$ ), implying a mean detection age of 76 years.

### 3.5 Validation of the Gompertz model with fixed expansion time in an external cohort

The French group of MPN recently developed a national database on ET and PV (BCB-FIMBANK: French National Cancer Institute (INCa) BCB 2013 and 2022, CHU Angers) (Table 2). We considered that this database is representative of the general population given the data size (1111 JAK2V617F MPN patients) (see Figure 1 **C-D** for the histogram before and after death adjustment), even if it is not as exhaustive as the previous database that reported all the cases in the region. We used this second data set to validate the Gompertz model with fixed expansion time (7). We performed an estimation of the parameters through the same EM algorithm as previously described and then applied a Chi-Square goodness-of-fit test, which was not rejected with a power of 0.99 (see Figure 6). This proposed model seems to properly explain MPN emergence and proliferation given our two data sets. This suggests that not only the mutation rate cannot be constant through life, but increases exponentially with age following the Gompertz model. Given these positive results to fit the data, we used the Gompertz model with fixed expansion time to compare the differences in mutation acquisition and expansion between the two pathologies PV and ET.

### 3.6 Differential analysis of Essential thrombocytemia and polycythemia Vera

We hypothesized that ET and PV have a different kinetic because of the double hit in PV compared to single hit in ET: homologous recombination or development of secondary mutations that induces the polycythemia instead of the thrombocytosis only. Given the high number of reported MPN in the FIMBANK cohort, we use this data set to analyze the difference between ET and PV patients.

There is not a clear difference between the two diseases data (see Figure 7). Yet, when looking at their means and standard deviations (see Table 3), PV presents a bigger mean by 2 years than ET. The standard deviation of ET is bigger by 1.6 years, meaning that the ages of detection are spread across a larger range. We started by testing if ET and PV corrected data come from the same distribution through a Chi-square test, which rejected this hypothesis with a p-value of  $10^{-11}$ . Hence, we confirmed that the diagnostic age distributions are different for ET and PV (at a 99% confidence level).

We proceeded to estimate the parameters of each pathology under the Gompertz model with fixed expansion time (7) and found the following values for the parameters, the mean ( $m_1$ ) and

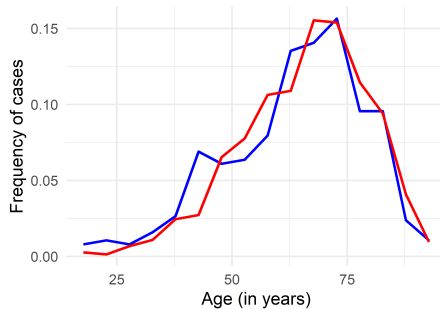


Figure 7: Frequencies of JAK2V617F ET (red line) and JAK2V617F PV (blue line) by age at diagnosis in the National BCB-FIMBANK Cohort

standard deviation ( $s_1$ ) of  $T_1$  for each disease

$$\begin{aligned}
 A^{PV} &= 0.00037, & k^{PV} &= 0.08575, & T_2^{PV} &= 8.8, & m_1^{PV} &= 56.9, & s_1^{PV} &= 14.2 \\
 A^{ET} &= 0.00056, & k^{ET} &= 0.07935, & T_2^{ET} &= 8.3, & m_1^{ET} &= 55.5, & s_1^{ET} &= 15.1.
 \end{aligned}$$

The estimation under our model indicates that the average mutation occurrence time ( $T_1$ ) is approximately 1.5 years higher for PV which could be explained by the time taken for the mitotic recombination to happen.

## 4 Discussion

Our present work provides mathematical modeling of JAK2V617F MPN emergence and expansion based on real life incidence and age at diagnosis, which highlights the role of an exponential age dependence increase of mutation occurrence in MPN. Based on the regional exhaustive registry of Côte d’Or (France), and lastly validated in a MPN national registry (BCB-FIMBANK registry), we modelled the occurrence and expansion times of JAK2V617F MPN. Most of the previous works performed to decipher the time of JAK2V617F “first” cell appearance, are based on genetic hierarchy and back-tracking performed on ancient blood samples or bone marrow samples (see [4], [5], [6]). These genetic approaches rely upon premises of a rate (a frequency) of mutation occurrence as yet unknown in MPN. It necessitates old blood or bone marrow samples for genetic analysis (to recapitulate the genetic tree evolution of the initial cancer cell) which is obviously very rare and probably biased [18]. Genetic analysis inference performed in such approaches are based on mutation appearance but not necessary proliferative/oncogenic. Indeed, it is now well documented that such JAK2V617F mutations could stay for long time without development of pathologies, as seen in clonal hematopoiesis of indeterminate potential (CHIP). Moreover, these genetic back-tracking approaches were built on stable mutation frequencies that overestimate the time of emergence if mutation rate during life is not constant. Our approach was based on registry analysis, differing from classical genetic back-tracking of mutation emergence and we showed that not only the mutation rate cannot be constant, but needs to grow exponentially with age, following the well known Gompertz model. We assumed that two periods of time were necessary to develop and diagnose MPN: a first time period ( $T_1$ ) corresponding to the mutation acquisition (genetic event from the conception of the embryo) but also its activation (ie ensuring to develop). This first period of time can correspond biologically to a cell cycle entry of a long-lasting quiescent cell for example, but also includes the possibility of a MPN cancer cell to disappear due to the cancer cell extinction probability. The second time period ( $T_2$ ) corresponds to the growth and development of such cancer stem cell until diagnosis. This type of modeling has been applied to invasion-fixation of mutants in eco-evolutionary models (see [19], [20]) and to the infectious diseases propagation (see [21], [22]) but less frequently to cancer emergence and development. Most reported modeling assumes that mutation and invasion rate are aging independent (ie a fixed rate of mutation and activation and a fixed probability of emergence of the pathology for a

given patient), which would imply that  $T_1$  follows an exponential law. However, models under this hypothesis show a peak of cases in younger ages, which is not coherent with the data, where most cases are present for older ages. We then speculated that myeloproliferative neoplasm emergence could need an age-dependent modeling for  $T_1$ . Age dependence does not necessarily mean that the JAK2V617F mutation acquisition is higher in aged stem cells than in young ones; it also could be interpreted as a mutation appearance during childhood or even before birth, but an activation due to external stimulus long time after. The second time (expansion time) is easier to characterize. A model considering the expansion time as a fixed value properly fits the data and is chosen over one as a random variable. This suggests that external changes (stress, food, toxic exposure...) could not significantly modify the behavior of MPN development and that the proliferation time from one “active” cancer cell to the total mass of cancer at diagnosis is relatively fixed. This could mean that the main determining factor is the proliferative speed related to the mutation acquisition. We then can speculate about the possibility (and risks and benefits) to treat subjects with JAK2V617F clonal hematopoiesis to delay the emergence of the MPN or prevent the classical thrombotic complications related to these pathologies. Our mathematical and statistical study allows us to assess the time of emergence and development of MPN. We found that the mean time for cancer cell to emerge is 63 years and time from tumor emergence to diagnosis is approximately 8.8 years in accordance with previous hypothesis, (see [23] and [24]). Based on the Variant Allele Frequency of JAK2V617F in the “FIMBANK” cohort, we observe that the mean JAK2V617F VAF in MPN is around 30% (19.9% in ET and 46.1% in PV respectively) and an increased ratio of 1.4% per year (as reported previously in untreated [25] or Hydroxyurea only treated patients [26]). This should mean a 10-year period of time from undetectable VAF to the 30% allele ratio observed at diagnosis in our MPN cohort. This is very close (and a little bit higher) to the 8.8 years of tumor expansion time to MPN diagnosis that we calculated in our model. Furthermore, our modeling fits well with the JAK2V617F CHIP that has been described to take approximately a decade to transform to MPN [27], [28], [29]. In conclusion, we demonstrated using mathematical modelling that the emergence and fixation of JAK2V617F mutation is strongly linked to aging mechanisms and that the expansion time of MPN can be considered as non random. Our numerical results show a mean of 63.1 years for the emergence and fixation of the mutation, and an expansion time of approximately 8.8 years. Altogether, these results highlight the interest to test all 50-60 years-old inhabitants for JAK2V617F CHIP and the place of preventive therapies for such subjects.

## References

- [1] W. Vainchenker and R. Kralovics. “Genetic basis and molecular pathophysiology of classical myeloproliferative neoplasms”. In: *Blood* 129.6 (2017), pp. 667–679.
- [2] A. Tefferi and J.W. Vardiman. “Classification and diagnosis of myeloproliferative neoplasms: The 2008 World Health Organization criteria and point-of-care diagnostic algorithms”. In: *Leukemia* 22.1 (2008), pp. 14–22.
- [3] L. M. Scott et al. “Progenitors homozygous for the V617F mutation occur in most patients with polycythemia vera, but not essential thrombocythemia”. In: *Blood* 108.7 (2006), pp. 2435–2437.
- [4] F. Osorio et al. “Somatic mutations reveal lineage relationships and age-related mutagenesis in human hematopoiesis”. In: *Cell Reports* 25 (2018), pp. 2308–2316.
- [5] D. Van Egeren et al. “Reconstructing the lineage histories and differentiation trajectories of individual cancer cells in myeloproliferative neoplasms”. In: *Cell Stem Cell* 28 (2021), pp. 514–523.
- [6] E. Mitchell et al. “Clonal dynamics of haematopoiesis across the human lifespan”. In: *Nature* 606 (2022), pp. 343–350.
- [7] G. Hermange et al. “Inferring the initiation and development of myeloproliferative neoplasms”. In: *PNAS* 119 (2022).

- [8] M. Rohrbacher et al. “Clinical trials underestimate the age of chronic myeloid leukemia (CML) patients. Incidence and median age of Ph/BCR-ABL-positive CML and other chronic myeloproliferative disorders in a representative area in Germany”. In: *Leukemia* 23 (2009), pp. 602–604.
- [9] O. Moulard et al. “Epidemiology of myelofibrosis, essential thrombocythemia, and polycythemia vera in the European Union”. In: *European Journal of Haematology* 92.4 (2014), pp. 289–297.
- [10] INED. *Data from "taux de mortalité par sexe et age INED"*. Available at <https://www.ined.fr/fr/tout-savoir-population/chiffres/france/mortalite-cause-deces/taux-mortalite-sexe-age>. 2021.
- [11] Matthieu Mosca et al. “Inferring the dynamic of mutated hematopoietic stem and progenitor cells induced by IFN -  $\alpha$  in myeloproliferative neoplasms”. In: *American Society of Hematology* (2021).
- [12] M. Lavielle. *Mixed Effects Models for the population Approach: Models, Tasks, Methods and Tools*. Second. 2014.
- [13] G. J. McLachlan and T. Krishnan. *The EM Algorithm and extensions*. Wiley-Interscience, 2008.
- [14] S. Rai and D. Matthews. “Improving the EM algorithm”. In: *Biometrics* 46 (1993), pp. 587–591.
- [15] C. Finch, M. C. Pike, and M. Witten. “Slow mortality rate accelerations during aging in some animals approximate that of humans”. In: *Science* (1990).
- [16] R. Riffenburgh and P. Johnstone. *Survival patterns of cancer patients*. American Cancer Society, 2001.
- [17] G. Schwarz. “Estimating the Dimension of a Model”. In: *The Annals of Statistics* 6.2 (1978), pp. 461–464.
- [18] P. Hirsch et al. “Clonal history of a cord blood donor cell leukemia with prenatal somatic JAK2V617F mutation”. In: *Leukemia* 30 (2016), pp. 1756–1759.
- [19] N. Champagnat, R. Ferrière, and S. Méléard. “Unifying evolutionary dynamics: From individual stochastic processes to macroscopic models”. In: *Theoretical Population Biology* 69 (2006), pp. 297–321.
- [20] S. Billiard and C. Smadi. “The interplay of two mutations in a population of varying size: a stochastic eco-evolutionary model for clonal interference”. In: *Stochastic Processes and their Applications* 127 (2017), pp. 701–748.
- [21] A. D. Barbour et al. “Escape from the boundary in markov population processes”. In: *Advances in Applied Probability* 47 (2015), pp. 1190–1211.
- [22] A. Barbour and G. Reinert. “Approximating the epidemic curve”. In: *Electronic Journals of Probability* 18 (2013), pp. 1–30.
- [23] T. Radivoyevitch et al. “Quantitative modeling of chronic myeloid leukemia: insights from radiobiology”. In: *Blood* 119 (2012), pp. 4363–4671.
- [24] T. McKerrell et al. “JAK2 V617F hematopoietic clones are present several years prior to MPN diagnosis and follow different expansion kinetics”. In: *Blood Advances* 1 (2017), pp. 968–971.
- [25] B. Stein et al. “Sex differences in the JAK2 V617F allele burden in chronic myeloproliferative disorders”. In: *Haematologica* 95 (2010), pp. 1090–1097.
- [26] J.-J. Kiladjian et al. “Long-term outcomes of polycythemia vera patients treated with ropeginterferon alfa-2b”. In: *Leukemia* 36 (2022), pp. 1408–1411.
- [27] C. Nielsen et al. “The JAK2 V617F somatic mutation, mortality and cancer risk in the general population”. In: *Haematologica* 96 (2011), pp. 450–453.
- [28] C. Nielsen et al. “Diagnostic value of JAK2 V617F somatic mutation for myeloproliferative cancer in 49,488 individuals from the general population”. In: *British Journal of Haematology* 160 (2013), pp. 70–79.

- [29] I. A. van Zeventer et al. “Evolutionary landscape of clonal hematopoiesis in 3,359 individuals from the general population”. In: *Cancer Cell* 41 (2023), pp. 1017–1031.

## Tables

Age	PMF	PV JAK2+	ET JAK2+	Total JAK2+ cases
0 to 4	0	0	0	0
5 to 9	0	0	0	0
10 to 14	0	0	0	0
15 to 19	0	0	0	0
20 to 24	0	0	0	0
25 to 29	0	0	0	0
30 to 34	0	1	4	5
35 to 39	0	0	4	4
40 to 44	0	1	4	5
45 to 49	0	5	4	9
50 to 54	0	2	7	9
55 to 59	1	8	11	20
60 to 64	1	10	6	17
65 to 69	2	13	15	30
70 to 74	4	12	14	30
75 to 79	5	14	29	48
80 to 85	4	15	30	49
More than 85	4	11	23	38
Total number	21	92	151	264

Table 1: First data set (Côte d'Or).

Age	PV JAK2+	ET JAK2+	Total JAK2+ cases
0 to 4	0	0	0
5 to 9	0	0	0
10 to 14	0	0	0
15 to 19	2	3	5
20 to 24	1	4	5
25 to 29	5	3	8
30 to 34	8	6	14
35 to 39	18	10	28
40 to 44	20	26	46
45 to 49	48	23	71
50 to 54	57	24	81
55 to 59	78	30	108
60 to 64	80	51	131
65 to 69	114	53	167
70 to 74	113	59	172
75 to 79	84	36	120
80 to 84	69	36	105
85 to 90	30	9	39
90 to 94	7	4	11
Total number	734	377	1111

Table 2: Second data set (FIMBANK).

		Number of cases	Mean age at diagnosis	Standard deviation of age	VAF JAK2 at diagnosis	Standard deviation of VAF
PV	Female	314	66.7	13.7	45.3	22.9
	Male	421	64.0	13.3	46.7	30.3
ET	Female	229	63.0	15.9	19.2	5.7
	Male	147	63.2	13.8	20.9	15.8

Table 3: Information concerning the pathologies PV versus ET by sex.